CHEMISTRY
A EUROPEAN JOURNAL

FULL PAPER

DOI: 10.1002/chem.201201365

Bulge-like Asymmetric Heterodye Clustering in DNA Duplex Results in Efficient Quenching of Background Emission Based on the Maximized Excitonic Interaction

Taiga Fujii,[a] Yuichi Hara,[a] Takuya Osawa,[a] Hiromu Kashida,*[a, b] Xingguo Liang,[a, b] Yasuko Yoshida,[b] and Hiroyuki Asanuma*[a, b]

Abstract: Asymmetric dye clusters with a single fluorophore (Cy3) and multiple quenchers (4′-methylthioazobenzene-4-carboxylate, methyl red, and 4′-dimethylamino-2-nitroazobenzene-4-carboxylate) were prepared. The dye and one-to-five quenchers were tethered through D-threoninol to opposite strands of a DNA duplex. NMR analysis revealed that the clusters with a single fluorophore and two quenchers formed a sandwich-like structure (antiparallel H-aggregates). The melting temperatures of all the heteroclusters were almost the same, although structural distortion should become larger, as the number of quenchers increased. An asymmetric heterocluster of a single fluorophore and two quenchers showed larger excitonic interaction (i.e., hypochromicity of Cy3), than did a single Cy3 and a single quencher. Due to the larger exciton coupling between the dyes, the 1:2 heterocluster suppressed the background emission more efficiently than the 1:1 cluster. However, more quenchers did not enhance quenching efficiency due to the saturation of exciton coupling with two quenchers. Finally, this asymmetric 1:2 heterocluster was introduced into the stem region of a molecular beacon (MB; also known as an in-stem MB) targeting the fusion site in the L6 *BCR-ABL* fusion gene. With this MB design, the signal/background ratio was as high as 68 due to efficient suppression of background emission resulting from the maximized excitonic interaction.

Keywords: cluster compounds · coherent quenching · DNA · dyes/pigments · NMR spectroscopy

Introduction

The excitonic interaction is a static interaction among closely stacked dye molecules[1] that induces narrowing of the absorption band and a bathochromic or a hypsochromic shift depending on stacking geometry.[2] H- and J-bands that show large hypsochromicity and bathochromicity due to vertical and stair-like stacking, respectively, are typical examples of effects of excitonic interactions.[2–3] UV/Vis spectra depend on the size of the dyes as well as their mutual orientations. Notably, in homodye clusters, exciton coupling among the cluster (spectroscopic aggregation number or coherence length) is saturated with 10–20 dye molecules at room temperature.[4] The relationship between cluster size and excitonic interaction in heteroclusters of different dyes has scarcely been investigated due to the difficulty of their preparation.[5] Especially, only a limited number has been reported on the exciton coupling between a dye and the other dyes (1:*n* type heteroclusters).

Recently, DNA and RNA have been used as scaffolds to prepare organized assemblies of dyes: nucleic acid scaffolds allow control of the number of the dyes in an array and of their mutual orientation.[6] For example, Matray and Kool reported oligofluorosides composed of fully artificial base surrogates tethered to fluorophores: these single-stranded scaffolds based on the D-ribose were used to prepare various functional heteroclusters.[7] Häner and co-workers developed heteroclusters of dyes linked to dialkynylpylene–perylenediimide pairs that were introduced into DNA duplexes.[8] Wagenknecht and co-workers incorporated 3-amino-1,2-propanediols (C2 linkers) in a DNA duplex by placing abasic sites at the counterpart of the base surrogates to ensure interstrand helical assembly.[9] We have also developed a new methodology to prepare organized assemblies of homo- and heterodyes by using D-threoninol as a scaffold.[10] Introduction of base surrogates linked to dyes into the centers of two complementary DNAs resulted in a stacked H-type dye cluster in antiparallel manner in the duplex. Because it is difficult to prepare well-defined heterodye clusters, this method was applied first to verify molecular exciton theory

[a] Dr. T. Fujii, Y. Hara, T. Osawa, Dr. H. Kashida, Prof. Dr. X. Liang, Prof. Dr. H. Asanuma
Department of Molecular Design and Engineering
Graduate School of Engineering, Nagoya University
Furo-cho, Chikusa-ku, Nagoya 464-8603 (Japan)
Fax: (+81) 52-789-2528
E-mail: asanuma@mol.nagoya-u.ac.jp
kashida@mol.nagoya-u.ac.jp

[b] Dr. H. Kashida, Prof. Dr. X. Liang, Y. Yoshida, Prof. Dr. H. Asanuma
Innovative Research Center for PME
Nagoya University
Furo-cho, Chikusa-ku, Nagoya 464-8603 (Japan)

Supporting information for this article is available on the WWW under http://dx.doi.org/10.1002/chem.201201365.

of heteroclustered dyes from scientific point of view.[10f] With the exception of spectral shifts, experimental results qualitatively agreed with theoretical predictions. Thus, heterodimerization induced hyperchromism of the shorter wavelength band (in-phase transition), but hypochromism of the longer wavelength band. These absorbance changes were enhanced, when the $\Delta\lambda_{max}$ of the two dyes was decreased.

Next, our method was applied to design a type of highly sensitive molecular beacon (MB), the in-stem MB (ISMB), by introducing a heterodimer of fluorophore and quencher into the stem region of MB to facilitate the quenching of emission in the closed state.[11] Interestingly, as Johansson et al. proposed,[12] our systematic studies on the spectroscopic behavior of fluorophore–quencher dimer revealed that a stronger excitonic interaction between the dyes suppressed the background emission in the closed MB more efficiently and resulted in a higher signal/background (S/B) ratio. Further enhancement of excitonic interaction between the dyes should raise quenching efficiency, leading to highly sensitive detection of a target DNA. Herein, we incorporated a single fluorophore (Cy3) and several quenchers (azo dyes) on D-threoninols into a duplex (Scheme 1). We found that an asymmetric heterocluster of a single fluorophore and two quenchers suppressed the background emission more efficiently than single fluorophore and quencher pair due to the larger exciton coupling of the duplex with two quenchers. Based on this result, a highly sensitive ISMB was designed with asymmetric 1:2 heterocluster in the stem region.

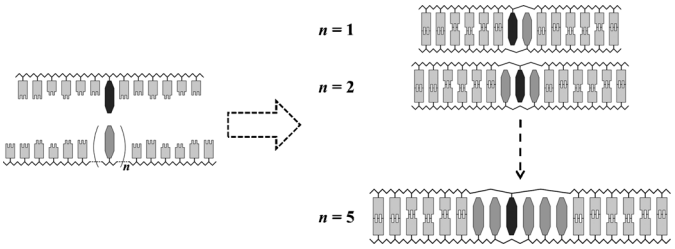

Scheme 1. Schematic illustration of the design of the asymmetric dye clusters by using D-threoninol as dye tethers. One strand with a fluorophore and the other strand with 1 to 5 quenchers (*n* denotes the number of the quenchers) were hybridized resulting in dye clustering.

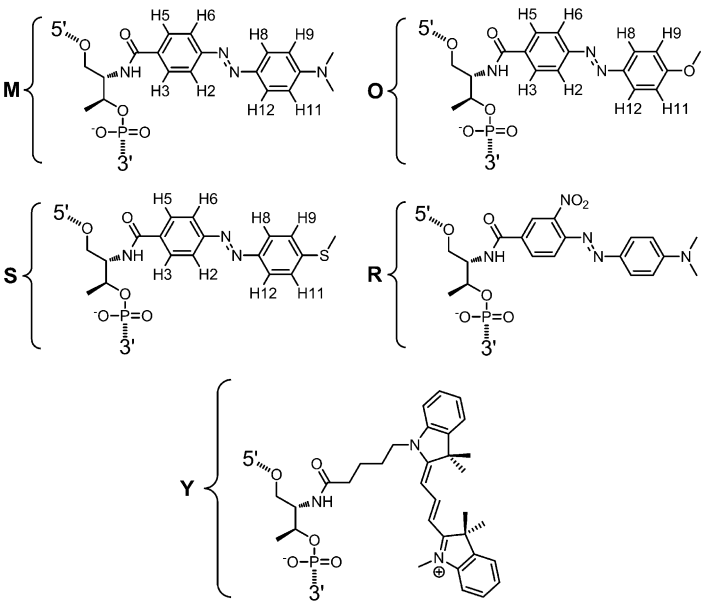

NMR-**MSa** : 5'-$C^1G^2A^3$-**MS**-$G^4T^5C^6$-3'
NMR-**Ob** : 3'-$G^{12}C^{11}T^{10}$-**O**-$C^9A^8G^7$-5'

N : 5'-GGT-ATC-GCA-ATC-3'
C : 3'-CCA-TAG-CGT-TAG-5'

Y1a : 5'-GGT-ATC-**Y**-GCA-ATC-3'
R*n*b : 3'-CCA-TAG-$\mathbf{R}_n$-CGT-TAG-5'
M*n*a : 5'-GGT-ATC-$\mathbf{M}_n$-GCA-ATC-3' ***n*** = 1-5
S*n*a : 5'-GGT-ATC-$\mathbf{S}_n$-GCA-ATC-3'
Y1b : 3'-CCA-TAG-**Y**-CGT-TAG-5'

T-MB : 5'-CA-GAG-TTC-AAA-AGC-CCT-TCA-3'
MB1 : 5'-TG-**Y**-GTC-*TGA-AGG-GCT-TTT-GAA-CTC-TG*-GAC-**R**-CA-3'
MB2 : 5'-TG-**Y**-GTC-*TGA-AGG-GCT-TTT-GAA-CTC-TG*-GAC-**RR**-CA-3'
MB3 : 5'-TGG-**Y**-TC-*TGA-AGG-GCT-TTT-GAA-CTC-TG*-GA-**R**-CCA-3'
MB4 : 5'-TGG-**Y**-TC-*TGA-AGG-GCT-TTT-GAA-CTC-TG*-GA-**RR**-CCA-3'

Scheme 2. Chemical structures and sequences of the ODNs synthesized in this study. In the MB sequences, the stem regions are underlined; the italicized region denotes the loop that recognizes the target sequence.

Results and Discussion

Structures and stabilities of duplexes with asymmetric dye clusters: Scheme 1 shows an illustration of a 1:*n* asymmetric dye cluster formed in the middle of the duplex. One strand has single dye and the other has consecutive dye residues at the center, and their hybridization affords a 1:*n* asymmetric dye cluster when the dyes are stacked with each other. Sequences of the DNAs incorporating dyes synthesized in this study are listed in Scheme 2. First, NMR analysis of a 1:2 heterocluster duplex was conducted to determine the alignment of the dyes, and then the stabilities of 1:*n* clustered duplexes were evaluated.

NMR analysis of 1:2 heterocluster: To discriminate proton signals of all the dye molecules in the duplex, three different dyes were introduced: 4′-dimethylaminoazobenzene-4-carboxylate (methyl red, **M**), 4′-methylthioazobenzene-4-carboxylate (**S**), and 4′-methoxyazobenzene-4-carboxylate (**O**). Two complementary strands, NMR-**MSa** and NMR-**Ob**, were synthesized (Scheme 2). NMR-**MSa** has **M** and **S** residues in the center, and NMR-**Ob** has an **O**. There are several possible alignments of the dyes as shown in Scheme 3.[13] The imino region ($\delta = 11.5$–14.0 ppm) of the 1D NMR spectrum of the duplex of these two strands recorded in H_2O is depicted in Figure 1. Signals corresponding to the six natural base pairs (C^1–G^{12}, G^2–C^{11}, A^3–T^{10}, G^4–C^9, T^5–A^8, and C^6–G^7) were assigned on the basis of NOESY and chemical shifts, indicating that the non-natural **M**, **S**, and **O** did not interrupt the base pairing.[14] Figure 2 depicts the NOEs between the imino-proton signal ($\delta = 11.5$–14.0 ppm) and the aromatic-proton signal ($\delta = 6.0$–6.7 ppm) regions. A distinct

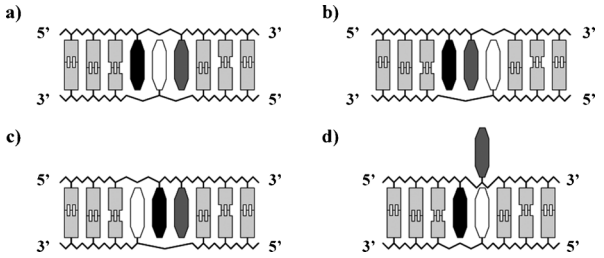

Scheme 3. Schematic illustration of four possible alignments of the asymmetric dye clusters. The dye (white) and quenchers (black and gray) are located on opposite strands. a) The dye is located between quenchers (corresponding to **M*O*S** orientation in NMR-**MSa**/NMR-**Ob**); b) natural nucleobases are to the 5′-side of the dye (corresponding to **MS*O*** orientation); c) natural nucleobase are to the 3′-side of the dye (corresponding to ***O*MS** orientation); or d) the dye or the quencher is flipped out from the duplexes.

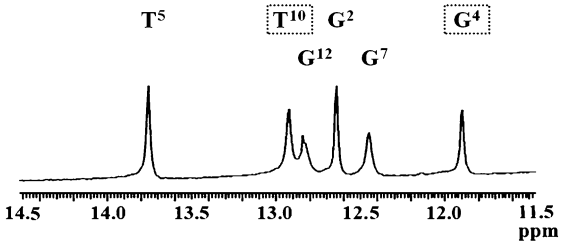

Figure 1. Imino region of the 1D NMR spectrum of the NMR-**MSa/**NMR-**Ob** duplex in H_2O/D_2O 9:1 at 278 K in phosphate buffer (20 mM, pH 7.0) and NaCl (200 mM). The duplex concentration was 1.0 mM. Assignments of the imino protons and the residue number are denoted above the peaks.

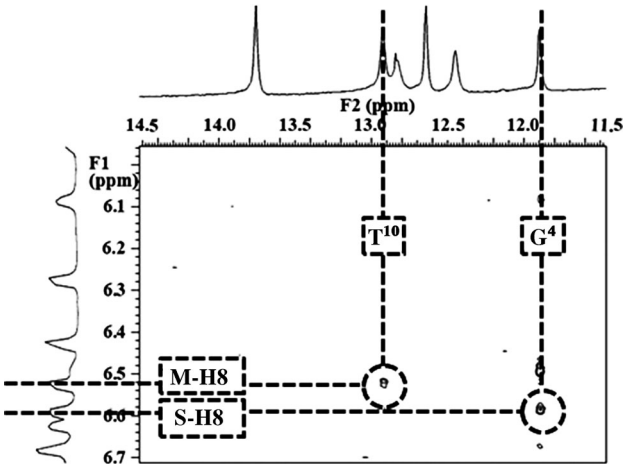

Figure 2. 2D NOESY spectrum (mixing time = 150 ms) between the imino-proton signals (δ = 11.5–14.5 ppm) and the aromatic-proton signals (δ = 6.0–6.7 ppm) for the NMR-**MSa/**NMR-**Ob** duplex in H_2O/D_2O 9:1 at 278 K in phosphate buffer (20 mM, pH 7.0) and NaCl (200 mM). Assignments of the methyl red (**M**) and 4′-methylthioazobenzene (**S**) protons are denoted on the 1D spectra (F1 axis) by using the numbers designated in Scheme 2. The NOE signals surrounded by broken circles demonstrate intercalation of the methyl red and 4′-methylthioazobenzene.

NOE signal was observed between the imino proton of T^{10} and H8 (H12) of the **M** protons, indicating that the **M** residue was located near T^{10}. The imino proton of G^4 did not have NOE to **M**, but was in close proximity to H8 (H12) of the **S** residue. Thus, we could unambiguously exclude the possibilities that the single dye (shown in Scheme 3 in white) stacks with a natural base (shown in Scheme 3, panels b and c).

Figure 3 shows the NOESY between the regions of δ = 5.0–8.0 and 1.6–3.0 ppm. Proton signals from the **O** residue were correlated only with those of **M** and **S** residues, and no

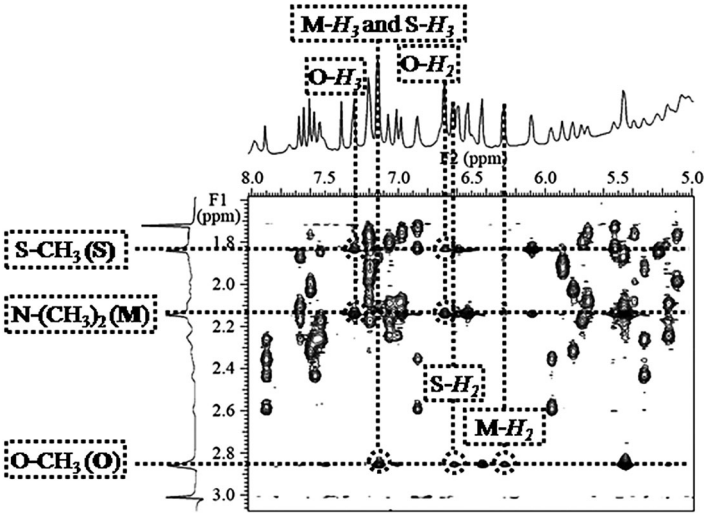

Figure 3. 2D NOESY spectrum (mixing time = 150 ms) between the regions of δ = 5.0–8.0 and 1.6–3.0 ppm for the NMR-**MSa/**NMR-**Ob** duplex in H_2O/D_2O 9:1 at 278 K in phosphate buffer (20 mM, pH 7.0) and NaCl (200 mM).

cross-peaks were observed between **M** and **S** residues as schematically shown in Figure 4a. Cross-peaks were observed between aromatic proton signals of **O**–H2 (**O**–H6) and **O**–H3 (**O**–H5) with those of both S–CH_3 of **S** and N–CH_3 of **M**. Moreover, relatively strong signals were also observed between O–CH_3 of **O** and aromatic protons of **M**–H2 (**M**–H6), **M**–H3 (**M**–H5), **S**–H2 (**S**–H6), and **S**–H3 (**S**–H5). These NOE signals indicate that **M**, **O**, and **S** were stacked as depicted in Figure 4a and in Scheme 3a: The **O** residue is sandwiched between **M** and **S** residues in the DNA duplex. The computer model of NMR-**MSa/**NMR-**Ob** was generated by using the InsightII/Discover3 software, and it is entirely consistent with the NMR analyses (Figure 4b).

Duplex stabilities of the asymmetric dye clusters: Introduction of several quencher dyes should induce a severe distortion of the duplex structure due to the increased asymmetry of the strands, which should affect the stability of the duplex. Thus, melting temperatures (T_m) of duplexes with 1 to 5 quenchers across from a single dye was measured (Table 1). In these experiments, the dye is not 4′-methoxyazobenzene (**O**), but rather Cy3 (**Y**); however, we assumed that a sandwich-type cluster was formed. Insertion of single **Y**–**R** pair (**Y1a**/**R1b**: 44.5 °C) slightly decreased the stability

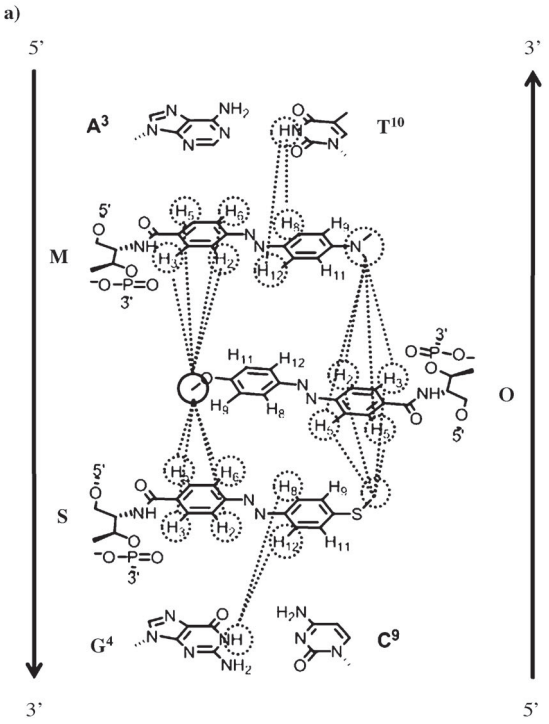

Figure 4. a) Stacking and orientations of **M**, **O**, and **S** residues in the duplex determined from NOESY. Broken lines indicate the observed NOE signals. b) Energy-minimized structure of the NMR-**MSa/**NMR-**Ob** duplex calculated with InsightII/Discover3 from the initial structure determined by NMR analyses. 4′-Methoxyazobenzene, 4′-methylthioazobenzene, and methyl red are shown in cyan, yellow, and red, respectively.

relative to the native duplex (**N/C**: 47.7 °C). The T_m of the cluster with a 1:2 bulge (**Y1a/R2b**: 44.8 °C) was almost same as that with a **Y**–**R** pair. Interestingly, addition of more **R** residues did not affect T_m significantly (46.1–47.1 °C,

Table 1. Effect of the number and quencher dyes on the melting temperature (T_m).[a]

	T_m [°C]		
	Y1a/R*n*b	**M*n*a/Y1b**	**S*n*a/Y1b**
N/C	47.7	–	–
$n=1$	44.5	45.3	46.2
$n=2$	44.8	46.0	48.2
$n=3$	46.1	47.5	49.2
$n=4$	47.1	48.2	50.0
$n=5$	47.1	49.3	49.1

[a] Solution conditions were as follows: [DNA] = 5 μM, [NaCl] = 100 mM, phosphate buffer (10 mM, pH 7.0).

Table 1), although distortion presumably increased dramatically. Similar results were observed when **M** or **S** was used as the quencher instead of **R**. These results are in contrast with our previous observation that asymmetric combinations of natural DNA with a strand containing a methyl red conjugate markedly destabilized the duplex.[10e,15] Presumably, stacking of Cy3 with quenchers linked through D-threoninols offset the destabilizing effect of the increased distortion.

Effect of the number of quenchers on excitonic interaction among the dyes: Next, the effect of the number of quencher dyes on excitonic interaction was investigated. To estimate the strength of exciton coupling, hypochromicity of Cy3 absorption by the quencher(s) was quantified by the comparison of UV/Vis spectrum of Cy3 before and after hybridization of quencher strand. Figure 5a shows typical excitonic interaction between Cy3 in **Y1a** and **R** in **R1b**. Each single-stranded **Y1a** (pink line) and **R1b** (purple line) gave absorption maxima at $\lambda = 549$ and 512 nm assigned to Cy3 and **R**, respectively, whereas hybridization of these two strands resulted in a blueshift (hypsochromicity) of the **R** band at $\lambda = 513$ nm and decrease in absorbance (hypochromicity) of Cy3 band at $\lambda = 550$ nm compared with the summed spectrum (blue line). Herein, the decrease in the absorbance (Figure 5a, black arrow) corresponds to the strength of the excitonic interaction, which was estimated as 0.32 (Table 2). An increase in the excitonic interaction was observed with **Y1a/R2b** (strength of excitonic interaction 0.47) as shown in Figure 5b and Table 2. However, introduction of additional quencher dyes did not significantly increase the interaction (Table 2 and Figure S1 in the Supporting Information), indicating that the excitonic interaction between **Y** and **R** was saturated with two quenchers. The other quenchers (methyl red and 4′-methylthioazobenzene) showed the same saturation behavior (Table 2, Figures S2 and S3 in the Supporting Information), although the maximum strength of the excitonic interaction depended on the dye.[16] Based on these results, we conclude that introduction of two quenchers results in the maximum excitonic interaction among a fluorophore and quenchers.

Quenching efficiency of a fluorophore: We previously reported that a larger excitonic interaction between a fluorophore and a quencher induced more efficient quenching of

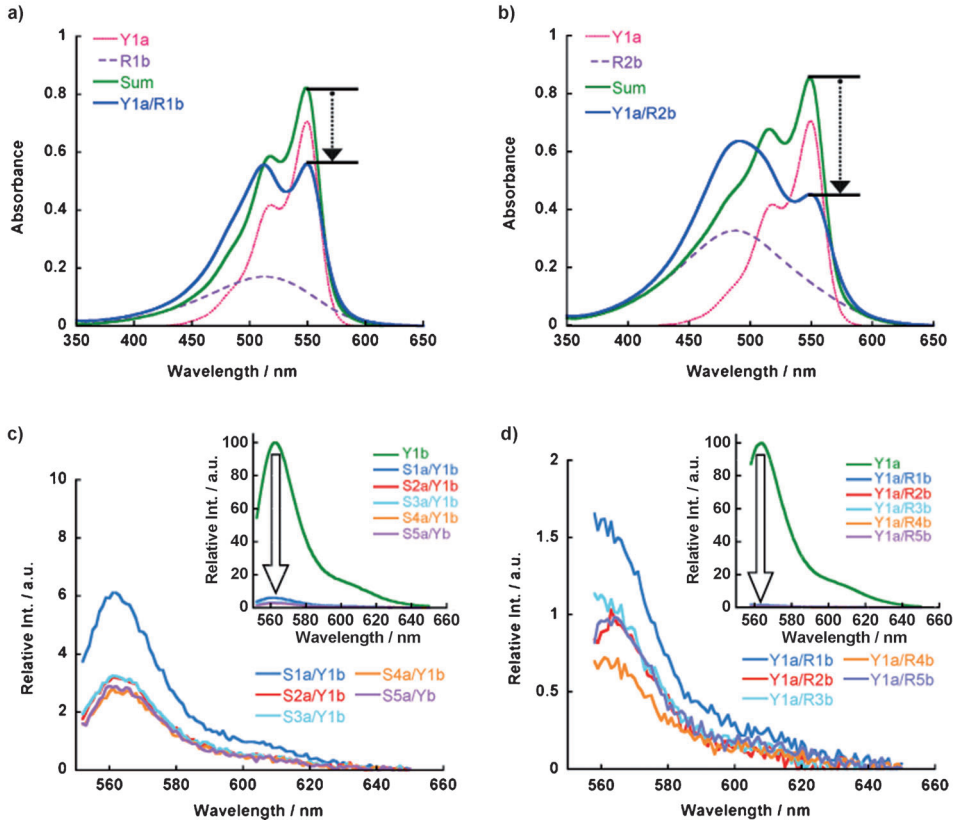

Figure 5. a) UV/Vis spectra of the **Y1a/R1b** duplex (blue line), single-stranded **Y1a** (pink dotted line), **R1b** (purple dashed line), and a simple sum of their spectra (green line); b) UV/Vis spectra of the **Y1a/R2b** duplex (blue line), single-stranded **Y1a** (pink dotted line), **R2b** (purple dashed line), and a simple sum of their spectra (green line). Hypochromicity (differences of absorbance of Cy3) before and after clustering were defined as strength of the exciton couplings (shown by dotted arrows). Solution conditions of UV/Vis spectra were DNA (5 μM), phosphate buffer (10 mM, pH 7.0), NaCl (100 mM); all spectra were recorded at 20 °C. Fluorescence emission spectra of Cy3 (**Y**) excited at $\lambda = 546$ nm and the duplexes containing c) 4′-methylthioazobenene and d) 4′-dimethylamino-2-nitroazobenzene as quenchers. DNA concentrations of fluorescence spectra were [**Sna**] = [**Rnb**] = 0.4 μM, [**Y1a**] = [**Y1b**] = 0.2 μM. Solutions contained phosphate buffer (10 mM, pH 7.0), NaCl (100 mM); all spectra were recorded at 20 °C.

Table 2. Effect of the number and type of quencher dye on the exciton couplings of the quenchers to a fluorophore and the quenching efficiencies.

	Y1a/Rnb		**Mna/Y1b**		**Sna/Y1b**	
	H[a,b]	QE[c] [%]	H[a,b]	QE[c] [%]	H[a,b]	QE[c] [%]
$n=1$	0.32	98.5	0.25	96.5	0.10	93.9
$n=2$	0.47	99.0	0.36	97.3	0.15	96.8
$n=3$	0.48	99.0	0.38	96.8	0.18	96.8
$n=4$	0.47	99.3	0.36	96.4	0.17	97.3
$n=5$	0.52	99.0	0.39	97.7	0.19	97.1

[a] Solutions contained DNA (5 μM), phosphate buffer (10 mM, pH 7.0), NaCl (100 mM); all spectra were recorded at 20 °C. [b] Hypochromicity (H) was evaluated from difference of absorbance between the heteroclusters and the sum spectrum of each single strand at Cy3 absorption region (**Y1a/Rnb**; $\lambda = 549$ nm, **Mna/Y1b**; $\lambda = 552$ nm, **Sna/Y1b**; $\lambda = 552$ nm). [c] Quenching efficiencies (QE) are the differences in fluorescent intensities between the clusters and the single strand with a Cy3 residue. The emission spectra of **Y1a/Rnb**, **Mna/Y1b**, and **Sna/Y1b** at $\lambda = 564$, 563, and 562 nm, respectively, excited at $\lambda = 546$ nm were used for these calculations. DNA concentrations were [**Mna**] = [**Sna**] = [**Rnb**] = 0.4 μM, [**Y1a**] = [**Y1b**] = 0.2 μM. Solutions contained phosphate buffer (10 mM, pH 7.0), NaCl (100 mM); all spectra were recorded at 20 °C.

the fluorophore.[11b] Emission spectra of **Sna/Y1b** and **Y1a/Rnb** are shown in Figure 5c and d. As shown in the insets, all clusters (**Y1a/Rnb** and **Sna/Y1b**) exhibited low fluorescence compared with that of single-stranded **Y1a** and **Y1b**. We found that two quenchers (**S2a/Y1b**) reduced emission more (96.8%) than a single quencher (**S1a/Y1b**; 93.9%). However, addition of more **S** residues did not significantly improve quenching efficiency. 4′-Dimethylamino-2-nitroazobenzene quenched Cy3 more efficiently than **S** due to the stronger excitonic interaction (compare blue lines in Figure 5d and c) as reported previously.[11b] However, more than two **R** residues did not further improve the quenching efficiency (Table 2). The same effect was also observed with methyl red (Figure S5 in the Supporting Information). We conclude that two consecutive quenchers maximized the quenching of a fluorophore due to the saturated excitonic interaction.

Design of highly sensitive in-stem MB: Based on the above quenching experiments, ISMBs[17] with two consecutive **R** residues as quenchers in the stem region, referred to as **MB2** and **MB4**, targeting a fusion site of L6 *BCR-ABL* fusion gene was designed.[18] Control ISMBs with single quencher, **MB1** and **MB3**, were also synthesized. Background emission of **MB2** was 56% lower than that of **MB1** in the absence of target (Figure 6a). Consequently, the S/B ratio, which was defined as the ratio of emission intensity of **MB2** in the presence versus absence of the target, is 68, whereas that of **MB1** is 27 (compare Figure 6b and c). This remarkable improvement of S/B ratio was also observed for **MB3** and **MB4** with the fluorophore–quencher pair at a different position in the ISMB (Figure S6 in the Supporting Information). Thus, highly sensitive ISMBs were successfully prepared by using the double-quencher design.

Conclusion

We have prepared asymmetric dye clusters in DNA duplexes by using D-threoninol as a scaffold for the dyes. In-stem

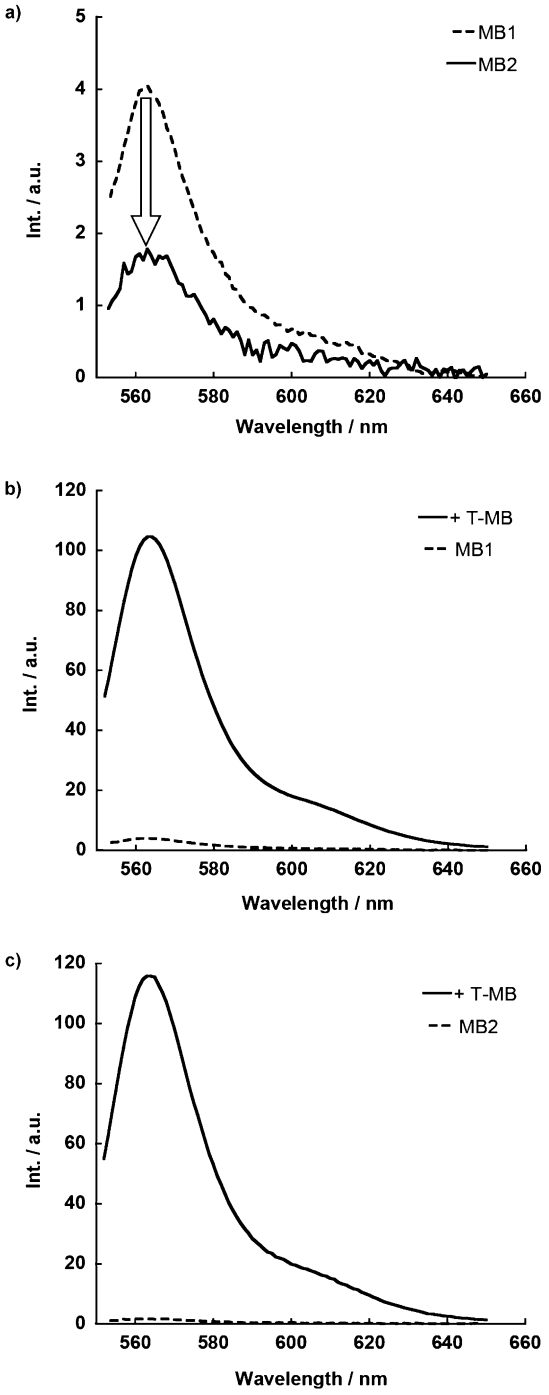

Figure 6. Fluorescence emission spectra of a) **MB1** (broken line) and **MB2** (solid line) excited at $\lambda = 546$ nm without **T-MB**; b) **MB1** with (solid line) and without (broken line) **T-MB**; and c) **MB2** with (solid line) and without (broken line) **T-MB**. DNA concentrations were [**T-MB**] = 0.4 μM, [**MB1**] = [**MB2**] = 0.2 μM. Solutions contained phosphate buffer (10 mM, pH 7.0), NaCl (100 mM); all spectra were recorded at 20 °C.

MB prepared by using a single fluorescent dye and two quenchers had quite low background emission. We are now applying this probe design to high-throughput detection of wild-type and chimeric gene expression associated with chronic myeloid leukemia in a microarray format and cells.[18]

Experimental Section

Materials: All conventional phosphoramidite monomers, CPG columns, reagents for DNA synthesis, and Poly-Pak II cartridges were purchased from Glen Research. Other reagents for the synthesis of phosphoramidite monomers were purchased from Tokyo Kasei and Sigma–Aldrich.

Synthesis of DNA modified with M, O, R, S, or Y: All the modified DNAs were synthesized by using an automated DNA synthesizer (ABI-3400 DNA synthesizer, Applied Biosystems) by using conventional and dye-carrying phosphoramidite monomers. 4′-Methylthioazobenzene, methyl red, and 4′-dimethylamino-2-nitroazobenzene phosphoramidite monomers were synthesized as reported previously.[10e,f] The compound 4′-methoxyazobenzene was synthesized according to the literature procedure.[19] Dyes were converted to phosphoramidite monomers as described in the Supporting Information, Scheme S1. The coupling efficiencies of the monomers with modified residues were as high as those of the conventional monomers as was judged from the intensity of the color of the released trityl cation. After work-up, the monomers were purified by reverse-phase HPLC and characterized by MS (MALDI-TOF; Autoflex II, Bruker Daltonics).

MS (MALDI-TOF) data: found versus calculated (calcd) for the monomers: **M1a**, found: 4062 (calcd for [***M1a***+H^+]: 4063); **M2a**: found 4481 (calcd for [***M2a***+H^+]: 4481); **M3a**: found 4899 (calcd for [***M3a***+H^+]: 4899); **M4a**: found 5318 (calcd for [***M4a***+H^+]: 5317); **M5a**: found 5735 (calcd for [***M5a***+H^+]: 5735); **S1a**: found 4067 (calcd for [***S1a***+H^+]: 4066); **S2a**: found 4488 (calcd for [***S2a***+H^+]: 4487); **S3a**: found 4909 (calcd for [***S3a***+H^+]: 4908). **S4a**: found 5332 (calcd for [***S4a***+H^+]: 5329); **S5a**: found 5752 (calcd for [***S5a***+H^+]: 5750); **R1b**: found 4108 (calcd for [***R1b***+H^+]: 4108); **R2b**: found 4572 (calcd for [***R2b***+H^+]: 4571); **R3b**: found 5034 (calcd for [***R3b***+H^+]: 5034); **R4b**: found 5501 (calcd for [***R4b***+H^+]: 5497); **R5b**: found 5966 (calcd for [***R5b***+H^+]: 5960); **Y1a**: found 4234 (calcd for [***Y1a***+H^+]: 4237); **Y1b**: found 4235 (calcd for [***Y1b***+H^+]: 4237); NMR-**MSa**: found 2630 (calcd for [*NMR-**MSa***+H^+]: 2632); NMR-**Ob**: found 2198 (calcd for [*NMR-**Ob***+H^+]: 2197); **MB1**: found 10300 (calcd for [***MB1***+H^+]: 10305). **MB2**: found 10772 (calcd for [***MB2***+H^+]: 10768); **MB3**: found 10302 (calcd for [***MB3***+H^+]: 10305); **MB4**: found 10769 (calcd for [***MB4***+H^+]: 10768).

Determination of molar extinction coefficients: Molar extinction coefficients for dye monomers at $\lambda = 260$ nm were determined by comparison of ratios between absorbances at $\lambda = 260$ nm and their λ_{max}.[20] These ratios were calculated from UV/Vis spectra of the dye monomers (such as compound **4** in Scheme S1 in the Supporting Information). The coefficients for dye monomers are listed in Table S1 in the Supporting Information.

Spectroscopic measurements: The UV/Vis spectra were measured on a JASCO model V-550 spectrophotometer and on a Shimadzu UV-1800 instrument in 10 mm quartz cells. Fluorescent spectra were measured with a JASCO model FP-6500 with a microcell. The excitation wavelength was 546 nm for Cy3. All models were equipped with programmable temperature controllers. All samples of DNA-dye conjugates were heated at 80 °C for 5 min in the dark to thermally isomerize the *cis*- to the *trans*-form before spectroscopic measurement.[21] Before fluorescent measurements of the MBs, all samples were cooled to 1 °C min^{-1} from 80 °C.

Measurement of melting temperatures: The melting curves of duplex DNAs were obtained by measurement of the change in absorbance at $\lambda = 260$ nm versus temperature. The melting temperature (T_m) was determined from the maximum of the first derivative of the melting curve. Both the heating and cooling curves were measured and the obtained T_m values were within 2.0 °C.

NMR measurements: DNA duplexes were lyophilized three times from buffer containing sodium phosphate (20 mM, pH 7.0) and then dissolved in the a H_2O/D_2O 9:1 solution or D_2O to give a duplex concentration of 1.0 mM. NaCl was added to give a final sodium concentration of 200 mM. NMR spectra were recorded with a Varian INOVA spectrometer (700 MHz) equipped for triple resonance at a probe temperature of 278 K. Resonances were assigned by standard methods by using a combi-

nation of 1D, total correlation spectroscopy (TOCSY, 60 ms mixing time), double-quantum filtered (DQF)-COSY, and NOESY (150 ms mixing time) experiments. All spectra in the H_2O/D_2O 9:1 solution were recorded by using the 3:9:19 WATERGATE pulse sequence for water suppression.[22]

Computer modeling: Molecular modeling by conformational energy minimization was performed with the InsightII/Discover3 software (Molecular Simulation, Inc.) on a Silicon Graphics O2+ workstation with the operating system IRIX64, release 6.5. An AMBER force field was used for the calculations. The results of the NMR analyses served as a starting point for the modeling. For the analysis a trimer of methyl red, 4′-methoxyazobenzene, and 4′-methylthioazobenzene, the trimer was prepared by positioning the three dye molecules in a cofacial orientation replacing three native base pairs.

Acknowledgements

This work was partially supported by a JSPS research fellowship for young scientists (to T.F.), a Grant-in-Aid for Scientific Research (A, 21241031), and a Grant-in-Aid for Young Scientists (B, 22750149) from the Ministry of Education, Culture, Sports, Science and Technology, Japan. Partial support by the SENTAN program, Japan Science and Technology Agency (JST) is also acknowledged.

[1] A. S. Davydov, *Theory of Molecular Excitons*, Plenum, New York, **1971**, p. 18.

[2] M. Kasha, *Radiat. Res.* **1963**, *20*, 55–70.

[3] *J-Aggregates* (Ed.: T. Kobayashi), World Scientific, Singapore, **1996**, pp. 1–40.

[4] a) M. van Burgel, D. A. Wiersma, K. Duppen, *J. Chem. Phys.* **1995**, *102*, 20–33; b) *J-aggregates* (Ed.: T. Kobayashi), World Scientific, Singapore, **1996**, p. 111–160; c) A. S. R. Koti, J. Taneja, N. Periasamy, *Chem. Phys. Lett.* **2003**, *375*, 171–176.

[5] a) K. Murata, S.-i. Kuroda, K. Saito, *Thin Solid Films* **1997**, *295*, 73–76; b) F. D. Lewis, Y. Wu, L. Zhang, X. Zuo, R. T. Hayes, M. R. Wasielewski, *J. Am. Chem. Soc.* **2004**, *126*, 8206–8215; c) F. D. Lewis, L. Zhang, X. Liu, X. Zuo, D. M. Tiede, H. Long, G. C. Schatz, *J. Am. Chem. Soc.* **2005**, *127*, 14445–14453; d) A. Yamaguchi, N. Kometani, Y. Yonezawa, *Thin Solid Films* **2006**, *513*, 125–135; e) A. L. Burin, M. E. Armbruster, M. Hariharan, F. D. Lewis, *Proc. Natl. Acad. Sci. USA* **2009**, *106*, 989–994; f) V. Czikkely, G. Dreizler, H. D. Försterling, H. Kuhn, J. Sondermann, P. Tillmann, J. Z. Wiegand, *Z. Naturforsch.* **1969**, *24a*, 1821–1830.

[6] a) J. L. Seifert, R. E. Connor, S. A. Kushon, M. Wang, B. A. Armitage, *J. Am. Chem. Soc.* **1999**, *121*, 2987–2995; b) M. Wang, G. L. Silva, B. A. Armitage, *J. Am. Chem. Soc.* **2000**, *122*, 9977–9986; c) S. Bernacchi, Y. Mély, *Nucleic Acids Res.* **2001**, *29*, 62e; d) R. A. Garoff, E. A. Litzinger, R. E. Connor, I. Fishman, B. A. Armitage, *Langmuir* **2002**, *18*, 6330–6337; e) S. Bernacchi, E. Piémont, N. Potier, A. v. Dorsselaer, Y. Mély, *Biophys. J.* **2003**, *84*, 643–654; f) M. Hariharan, Y. Zheng, H. Long, T. A. Zeidan, G. C. Schatz, J. Vura-Weis, M. R. Wasielewski, X. Zuo, D. M. Tiede, F. D. Lewis, *J. Am. Chem. Soc.* **2009**, *131*, 5920–5929; g) T. M. Wilson, T. A. Zeidan, M. Hariharan, F. D. Lewis, M. R. Wasielewski, *Angew. Chem.* **2010**, *122*, 2435–2438; *Angew. Chem. Int. Ed.* **2010**, *49*, 2385–2388; h) A. L. Stadler, B. R. Renikuntla, D. Yaron, A. S. Fang, B. A. Armitage, *Langmuir* **2011**, *26*, 1472–1479.

[7] a) T. J. Matray, E. T. Kool, *J. Am. Chem. Soc.* **1998**, *120*, 6191–6192; b) J. Gao, C. Strässler, D. Tahmassebi, E. T. Kool, *J. Am. Chem. Soc.* **2002**, *124*, 11590–11591; c) J. N. Wilson, Y. N. Teo, E. T. Kool, *J. Am. Chem. Soc.* **2007**, *129*, 15426–15427; d) S. S. Tan, S. J. Kim, E. T. Kool, *J. Am. Chem. Soc.* **2011**, *133*, 2664–2671.

[8] a) H. Bittermann, D. Siegemund, V. L. Malinovskii, R. Häner, *J. Am. Chem. Soc.* **2008**, *130*, 15285–15287; b) V. L. Malinovskii, F. Samain, R. Häner, *Angew. Chem.* **2007**, *119*, 4548–4551; *Angew. Chem. Int. Ed.* **2007**, *46*, 4464–4467; c) A. L. Nussbaumer, D. Studer, V. L. Malinovskii, R. Häner, *Angew. Chem.* **2011**, *123*, 5604–5608; *Angew. Chem. Int. Ed.* **2011**, *50*, 5490–5494; d) S. M. Biner, D. Kummer, V. L. Malinovskii, R. Haner, *Org. Biomol. Chem.* **2011**, *9*, 2628–2633.

[9] a) C. Wagner, H.-A. Wagenknecht, *Org. Lett.* **2006**, *8*, 4191–4194; b) D. Baumstark, H.-A. Wagenknecht, *Chem. Eur. J.* **2008**, *14*, 6640–6645.

[10] a) H. Asanuma, K. Shirasuka, M. Komiyama, *Chem. Lett.* **2002**, *31*, 490–491; b) H. Asanuma, K. Shirasuka, T. Takarada, H. Kashida, M. Komiyama, *J. Am. Chem. Soc.* **2003**, *125*, 2217–2223; c) H. Kashida, H. Asanuma, M. Komiyama, *Angew. Chem.* **2004**, *116*, 6684–6687; *Angew. Chem. Int. Ed.* **2004**, *43*, 6522–6525; d) H. Kashida, M. Tanaka, S. Baba, T. Sakamoto, G. Kawai, H. Asanuma, M. Komiyama, *Chem. Eur. J.* **2006**, *12*, 777–784; e) H. Kashida, T. Fujii, H. Asanuma, *Org. Biomol. Chem.* **2008**, *6*, 2892–2899; f) T. Fujii, H. Kashida, H. Asanuma, *Chem. Eur. J.* **2009**, *15*, 10092–10102.

[11] a) H. Kashida, T. Takatsu, T. Fujii, K. Sekiguchi, X. Liang, K. Niwa, T. Takase, Y. Yoshida, H. Asanuma, *Angew. Chem.* **2009**, *121*, 7178–7181; *Angew. Chem. Int. Ed.* **2009**, *48*, 7044–7047; b) Y. Hara, T. Fujii, H. Kashida, K. Sekiguchi, X. Liang, K. Niwa, T. Takase, Y. Yoshida, H. Asanuma, *Angew. Chem.* **2010**, *122*, 5634–5638; *Angew. Chem. Int. Ed.* **2010**, *49*, 5502–5506.

[12] a) M. K. Johansson, H. Fidder, D. Dick, R. M. Cook, *J. Am. Chem. Soc.* **2002**, *124*, 6950–6956; b) M. K. Johansson, R. M. Cook, *Chem. Eur. J.* **2003**, *9*, 3466–3471.

[13] Because the melting temperature of the NMR-**MSa**/NMR-**Ob** duplex was determined to be 25.6 °C, NMR measurements were performed at 5 °C (278 K), at which temperature a stable duplex is formed. To monitor imino protons that are exchangeable with water molecules, NMR spectra were recorded in H_2O/D_2O 9:1, with a 3:9:19 WATERGATE pulse sequence for H_2O suppression. When these data were combined with the NOESY, DQF-COSY, and TOCSY spectra, most of the signals of the duplex could be assigned.

[14] The imino-proton signals of the terminal G^7 and G^{12} were slightly broad because of the rapid exchange with water, whereas signals from the other residues remained sharp.

[15] The T_m of **M5a/C**, which was reported in the previous paper (see Ref. [10b]), was 36.3 °C under the buffer conditions used. This large destabilization was considered to be induced by the structural distortion. Thus, introduction of the dye residue (**Y**) on D-threoninol into the complementary strand significantly stabilized the duplexes.

[16] An increase in the number of quenchers induced hypsochromicity of quencher band (see Figure S4 in the Supporting Information).

[17] For highly sensitive molecular beacons, see: a) O. Seitz, *Angew. Chem.* **2000**, *112*, 3389–3392; *Angew. Chem. Int. Ed.* **2000**, *39*, 3249–3252; b) S. Tyagi, S. A. E. Marras, F. R. Kramer, *Nat. Biotechnol.* **2000**, *18*, 1191–1196; c) B. Dubertret, M. Calame, A. J. Libchaber, *Nat. Biotechnol.* **2001**, *19*, 365–370; d) H. Du, M. D. Disney, B. L. Miller, T. D. Krauss, *J. Am. Chem. Soc.* **2003**, *125*, 4012–4013; e) C. J. Yang, H. Lin, W. Tan, *J. Am. Chem. Soc.* **2005**, *127*, 12772–12773; f) C. J. Yang, M. Pinto, K. Schanze, W. Tan, *Angew. Chem.* **2005**, *117*, 2628–2632; *Angew. Chem. Int. Ed.* **2005**, *44*, 2572–2576; g) L. Wang, C. J. Yang, C. D. Medley, S. A. Benner, W. Tan, *J. Am. Chem. Soc.* **2005**, *127*, 15664–15665; h) C. Crey-Desbiolles, D.-R. Ahn, C. J. Leumann, *Nucleic Acids Res.* **2005**, *33*, e77; i) D. M. Kolpashchikov, *J. Am. Chem. Soc.* **2006**, *128*, 10625–10628; j) Y. Kim, C. J. Yang, W. Tan, *Nucleic Acids Res.* **2007**, *35*, 7279–7287; k) T. N. Grossmann, L. Röglin, O. Seitz, *Angew. Chem.* **2007**, *119*, 5315–5318; *Angew. Chem. Int. Ed.* **2007**, *46*, 5223–5225; l) E. Socher, L. Bethge, A. Knoll, N. Jungnick, A. Herrmann, O. Seitz, *Angew. Chem.* **2008**, *120*, 9697–9701; *Angew. Chem. Int. Ed.* **2008**, *47*, 9555–9559; m) S. Nakayama, L. Yan, H. O. Sintim, *J. Am. Chem. Soc.* **2008**, *130*, 12560–12561; n) E. Socher, D. V. Jarikote, A. Knoll, L. Röglin, J. Burmeister, O. Seitz, *Anal. Biochem.* **2008**, *375*, 318–330; o) S. Berndl, H.-A. Wagenknecht, *Angew. Chem.* **2009**, *121*, 2454–2457; *Angew. Chem. Int. Ed.* **2009**, *48*, 2418–2421; p) S. Kummer, A. Knoll, E. Socher, L. Bethge, A. Herrmann, O. Seitz, *Angew. Chem.* **2011**, *123*, 1972–1975; *Angew. Chem. Int. Ed.* **2011**, *50*, 1931–1934;

q) C. Holzhauser, H.-A. Wagenknecht, *Angew. Chem.* **2011**, *123*, 7406–7410; *Angew. Chem. Int. Ed.* **2011**, *50*, 7268–7272.
[18] a) H. Döhner, S. Stilgenbauer, K. Fischer, M. Schröder, M. Bentz, P. Lichter, *Stem Cells* **1995**, *13*, 76–82; b) C. Preudhomme, F. Révillion, A. Merlat, L. Hornez, C. Roumier, N. Duflos-Grardel, J. P. Jouet, A. Cosson, J. P. Peyrat, P. Fenaux, *Leukemia* **1999**, *13*, 957; c) C. L. Sawyers, *N. Engl. J. Med.* **1999**, *340*, 1330–1340; d) P. Bolufer, G. F. Sanz, E. Barragan, M. A. Sanz, J. Cervera, E. Lerma, L. Senent, I. Moreno, M. D. Planelles, *Haematologica* **2000**, *85*, 1248–1254.
[19] a) W. H. Nutting, R. A. Jewell, H. Rapoport, *J. Org. Chem.* **1970**, *35*, 505–508; b) M. A. Rahim, P. N. P. Rao, E. E. Knaus, *J. Heterocycl. Chem.* **2002**, *39*, 1309–1314.
[20] X. Liang, T. Mochizuki, H. Asanuma, *Small* **2009**, *5*, 1761–1768.
[21] H. Nishioka, X. Liang, H. Kashida, H. Asanuma, *Chem. Commun.* **2007**, 4354–4356.
[22] M. Liu, X.-a. Mao, C. Ye, H. Huang, J. K. Nicholson, J. C. Lindon, *J. Magn. Reson.* **1998**, *132*, 125–129.

Received: April 20, 2012
Published online: ■■ ▮▮, 0000

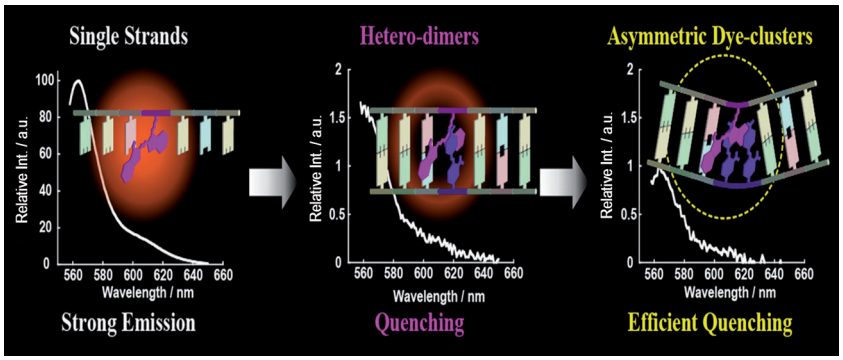

For reduction of the background emission with the DNA probes, asymmetric dye clusters were prepared by using D-threoninol as a dye–cluster scaffold in DNA. The cluster of single fluorophore and two quenchers suppressed the emission more efficiently than the heterodimer due to the strong exciton coupling between the dyes. This design was used to prepare a highly-sensitive in-stem molecular beacon (MB; see figure).

Asymmetric Dye Clusters

T. Fujii, Y. Hara, T. Osawa, H. Kashida, X. Liang, Y. Yoshida, H. Asanuma** ..... ▮▮▮▮–▮▮▮▮

Bulge-like Asymmetric Heterodye Clustering in DNA Duplex Results in Efficient Quenching of Background Emission Based on the Maximized Excitonic Interaction